APPLICATION OF SINGULAR PERTURBATION TECHNIQUES TO POWER SYSTEM TRANSIENT STABILITY ANALYSIS

by

Christopher L. DeMarco and Arthur R. Bergen

Memorandum No. UCB/ERL M84/7

20 February 1984

ELECTRONICS RESEARCH LABORATORY

College of Engineering
University of California, Berkeley
94720

Application of Singular Perturbation Techniques to Power System Transient Stabilty Analysis

Christopher L. DeMarco
Arthur R. Bergen

Department of Electrical Engineering and Computer Sciences
and the Electronics Research Laboratory
University of California, Berkeley, California 94720

ABSTRACT

This work extends Lyapunov techniques for power system transient stability analysis to system models incorporating voltage magnitude variation, real and reactive power loads, and flux decay effects. A method of estimating the domain of attraction of an asymptotically stable equilibrium in the resulting system of differential equations with algebraic constraints is examined using singular perturbation results.

Research sponsored by the Department of Energy contract DE-AC01-82-CE76221.

Application of Singular Perturbation Techniques to Power System Transient Stabilty Analysis

Christopher L. DeMarco
Arthur R. Bergen

Department of Electrical Engineering and Computer Sciences
and the Electronics Research Laboratory
University of California, Berkeley, California 94720

1. Introduction

Advances in the direct assessment of power system stability have addressed three related facets of the problem. The first is that of constructing a suitable Lyapunov or energy function, which is the basis of any direct method. The second area of interest is improved means of estimating stability boundaries given such a function. Finally, recent attempts have been made to improve the power system model to more accurately reflect observed system behavior. The work presented here primarily addresses the third issue, and as necessitated by our model, singular perturbation techniques are employed to obtain well defined system equations to which Lyapunov techniques may be applied.

Until recently, most applications of direct methods to multimachine power systems utilized classical synchronous machine models with pure impedance representations for loads. Such models cannot represent more general static or dynamic load behavior, nor generator flux decay and excitation dynamics. Several recent works have addressed these problems [4,14,20]. In [4], static nonlinear load models are employed with swing equations for both generators and loads. Hence voltage magnitude at load buses is allowed to vary according to constraints imposed by the static load models. A similar approach is taken in [14], where affine frequency dependent real power load and arbitrary static reactive power load models are used.

The drawbacks in the approaches of [4] and [14] lie in the models themselves. The combination of dynamic swing equations with static load models yields a system of differential equations with algebraic constraints. As we show in section 4, such a system is not in general well posed globally. This reflects the fact that static load models may not be applicable over the entire range of possible voltage variation. This problem is observed in [20], where it is suggested that the state space be restricted to those initial conditions from which trajectories of the system are well defined for all time. However, no method for identifying such a restricted state space is proposed, limiting the application of that work.

The application of singular perturbation results to power system stability studies was first examined in [18]. The results obtained concerned the local behavior of a system with fixed voltage magnitudes about its equilibrium points. In this work, we are concerned with stability in the large. For a model including voltage variation and flux decay effects, we construct a well posed augmented system of differential equations (no algebraic constaints). Using results of [13], we are able to explicitly characterize regions in which the augmented system "behaves like" the original model. We construct a Lyapunov function for the augmented system, and show that the region of attraction estimates obtained may be restricted to sets in which the augmented system and the original system are consistant. This provides an explicit technique to accomplish the goal suggested in [20]. From a broader perspective, this approach may be useful for obtaining estimates of the region of attraction for systems modelled by differential equations with algebraic constraints.

2. System Model

2.1. Network

Our analysis is an extension of the structure preserving model introduced in [5]. Assume the power system under consideration consists of $n_0 + 1$ buses (nodes), l_0 lines (branches) , and m generators. This physical network is augmented to include m buses representing internal voltage at each generator. These fictitious buses connect to the terminal buses through lines representing the generator transient reactance. The augmented network then consists of $n + 1$ buses, where $n = n_0 + m$, and $l = l_0 + m$ lines. We will choose an internal generator bus as reference, numbered 0, and number the remaining internal generator buses 1 through m-1, generator terminal buses m through 2m-1, and load buses 2m through n.

Because loads are not algebraically absorbed into the network as described in [8], it is reasonable to assume that the network is lossless. The resulting bus admittance matrix **Y** is pure imaginary, with elements $Y_{ik} = jB_{ik}$. We also assume slowly varying voltage magnitude and phase (quasi-steady-state). Hence voltage at a representative bus i will be given by a time varying phasor $V_i(t)$, with magnitude $|V_i|(t)$ and angle $\delta_i(t)$. Complex power absorded by the network at bus i is given by:

$$S_i = P_i + jQ_i = V_i(\mathbf{Y}\underline{V})^* \tag{1}$$

Transforming (1) to polar coordinates, it is convenient to define a vector of angle differences relative to the reference bus:

$$\underline{\alpha} \in \mathbf{R}^n \; ; \; \alpha_i = \delta_i - \delta_0$$

for i=1,2,...,n.

For convenience we define $\alpha_0 = 0$, with the understanding that α_0 is not a component of the system vector $\underline{\alpha}$. The load flow equations for the real and imaginary parts of S_i are then given by:

$$P_i = f_i(\underline{\alpha}, |\underline{V}|) = \sum_{k=0}^{n} |V_i||V_k| B_{ik} \sin(\alpha_i - \alpha_k) \tag{2}$$

$$Q_i = g_i(\underline{\alpha}, |\underline{V}|) = -\sum_{k=0}^{n} |V_i||V_k| B_{ik} \cos(\alpha_i - \alpha_k) \tag{3}$$

2.2. Load Models

2.2.1. Real Loads

As in the original structure preserving model, real loads are represented by affine functions of frequency. Empirical studies of loads with a significant induction motor component confirm that such a model is reasonable over a range of frequency variation of roughly 5% [1], consistant with our quasi-steady state assumption. In this formulation, we have real power absorbed by the load at bus i given by:

$$P_{l,i}+D_i\dot{\delta}_i \tag{4}$$

for i=m,m+1,...,n.

Observe that if P_i^0 is the equilibrium value of P_i given in (2), real power balance requires that $P_i^0 = -P_{l,i}$. Also, we will require that $D_i>0$.

2.2.2. Reactive Loads

Reactive power absorbed at bus i is modelled as either a Taylor expansion about the operating point (hence a polynomial in voltage magnitude) or an exponential function of voltage magnitude. We define:

$$q_i(|V_i|) = \begin{cases} q_i^0+q_i^1|V_i|+\cdots+q_i^r|V_i|^r \\ \text{or} \\ \beta\left(\frac{|V_i|}{|V_i^0|}\right)^\gamma \end{cases} \tag{5}$$

where q_i^0 through q_i^r or β,γ, and $|V_i^0|$ are parameters determined by load characteristics. We require $q_i^0 \geq 0$ and $\gamma \geq 1$.

Conservation of reactive power at bus i implies that $g_i(\underline{\alpha},|\underline{V}|)+q_i(|V_i|) = 0$. Under the assumption that $|V_i| \in \overset{\circ}{\mathbf{R}}_+$, i.e. bus voltage magnitudes are strictly positive, we may multiply by $|V_i|^{-1}$ to obtain:

$$|V_i|^{-1}\{g_i(\underline{\alpha},|\underline{V}|) + q_i(|V_i|)\} = 0 \tag{6}$$

for i=m,m+1,...,n.

2.3. Machine Models

Two generator representations are compatible with the Lyapunov function to be introduced in section 4; the well known classical model and a first order flux decay model. It will prove convenient to partition $|\underline{V}| \in \overset{\circ}{\mathbf{R}}_+^{n+1}$ as :

$$|\underline{V}| = \begin{bmatrix} |\underline{V}_1| \\ |\underline{V}_2| \end{bmatrix}$$

where $|\underline{V}_1| \in \overset{\circ}{\mathbf{R}}_+^m$ are internal bus voltages, components 0 through m-1, and $|\underline{V}_2| \in \overset{\circ}{\mathbf{R}}_+^{n-m+1}$ are terminal and load bus voltages, components m through n.

The classical model assumption of constant voltage magnitude behind transient reactance yields $|\underline{V}_1| = |\underline{V}_1^0|$, reducing system variables to $\underline{\omega}$, $\underline{\alpha}$, and $|\underline{V}_2|$. In the context of the classical model, we will simplify notation by dropping the subscript 2 whenever possible and let $|\underline{V}|$ denote the terminal and load bus voltage magnitudes. Internal generator bus voltage magnitudes will then be fixed parameters in the load flow equations (2) and (3).

The flux decay model is derived in appendix A. The resulting differential equation describing dynamics of the internal generator bus voltage magnitude is:

$$|\dot{V}_i| = \frac{1}{T'_{d0,i}}\left[E_{f,i}^0-|V_i|-\frac{x_{d,i}-x_{d,i}'}{x_{d,i}'}(|V_i|-|V_j|\cos(\alpha_i-\alpha_j))\right] \tag{7}$$

for i=0,1,...,m-1, where $|V_j|$ is the terminal bus voltage magnitude corresponding to generator i. Recalling that $B_{ij}=1/x_{d,i}'$ and $B_{ii}=-1/x_{d,i}'$, we may rewrite the right hand side of (7) in a form similar (6):

$$|\dot{V}_i| = -\left(\frac{x_{d,i}-x_{d,i}'}{T'_{d0}}\right)|V_i|^{-1}\left(g_i(\underline{\alpha},|\underline{V}|)+q_i(|V_i|)\right) \tag{8}$$

for i=0,1,...,m-1, where

$$q_i(|V_i|) = \frac{-E_{f,i}^0|V_i| + |V_i|^2}{x_{d,i}-xd'}$$

Thus far we have described the behavior of the internal generator bus voltage magnitudes. Dynamics of the bus voltage angles, $\underline{\alpha}$, are described by the well known swing equation:

$$M_i\dot{\omega}_i + D_{g,i}\omega_i + f_i(\underline{\alpha},|\underline{V}|)-P_{g,i} = 0 \tag{9}$$

for i=0,1,...m-1, where

M_i = generator inertia constant

$D_{g,i}$ = generator damping constant

$\omega_i = \dot{\delta}_i = \dot{\alpha}_i + \omega_0$

$P_{g,i}$ = mechanical input power

Conservation of real power implies $P_i^0 = P_{g,i}$, where P_i^0 is the steady state value of P_i as defined in (2) .

3. Degenerate System Equations

For both the classical and the flux decay generator representations, the models introduced in section 2 yield a system of differential equations with algebraic constraints. In the terminology of singular perturbation, these are "degenerate" systems, which we denote D .

Though the basic structure of the systems is the same for either representation, the details require separate treatment.

3.1. Classical Model

Here the system variables are $\underline{\omega}\in\mathbf{R}^m$, $\underline{\alpha}\in\mathbf{R}^n$, $|\underline{V}|=|\underline{V}_2|\in\overset{\circ}{\mathbf{R}}_+^{n-m+1}$. We define a vector function $\underline{h}:\mathbf{R}^n\mathrm{x}\overset{\circ}{\mathbf{R}}_+^{n-m+1}\rightarrow\mathbf{R}^{2n-m+1}$ by :

$$h_i = \begin{cases} f_i(\underline{\alpha},|\underline{V}|)-P_i^0 & i=1,2,\ldots,n \\ |V_j|^{-1}(g_j(\underline{\alpha},|\underline{V}|)+q_j(|V_j|)) & j=i-(n-m);\ i=n+1,\ldots,2n-m \end{cases}$$

We make the obvious partition of $\underline{h}$ as $\underline{h}_1(\underline{\alpha},|\underline{V}|)$ representing the first n components and $\underline{h}_2(\underline{\alpha},|\underline{V}|)$ representing the final n-m+1 components.

With these definitions, we may combine the scalar equations of section 2 to obtain:

$$\dot{\underline{\omega}} = -\mathbf{M}_g^{-1}\mathbf{D}_g\underline{\omega} - \mathbf{M}_g^{-1}\mathbf{T}_1{}^T\underline{h}_1(\underline{\alpha},|\underline{V}|) \tag{10a}$$

$$\dot{\underline{\alpha}} = \mathbf{T}_1\underline{\omega}-\mathbf{T}_2\mathbf{D}_l^{-1}\mathbf{T}_2{}^T\underline{h}_1(\underline{\alpha},|\underline{V}|) \tag{10b}$$

$$\underline{0} = \underline{h}_2(\underline{\alpha},|\underline{V}|) \tag{10c}$$

where

$$\mathbf{M}_g = diag[M_1, M_2, \ldots, M_m]$$
$$\mathbf{D}_g = diag[D_{g,0}, D_{g,1}, \ldots, D_{g,m-1}]$$
$$\mathbf{D}_l = diag[D_{l,m}, D_{l,m+1}, \ldots, D_{l,n}]$$
$$\mathbf{T} = [\mathbf{T}_1 | \mathbf{T}_2] = [-e \,|\, \mathbf{I}_{nxn}]$$
$$\mathbf{T}_1 \in \mathbf{R}^{nxm}\ ;\ \mathbf{T}_2 \in \mathbf{R}^{nxn-m+1};\ e = [1, 1, \ldots, 1]^T$$

3.2. Flux Decay Model

Here system variables are $\underline{\omega} \in \mathbf{R}^m, \underline{\alpha} \in \mathbf{R}^n$, and $|\underline{V}| = [|\underline{V}_1|^T, |\underline{V}_2|^T]^T \in \overset{\circ}{\mathbf{R}}_+^{n+1}$.

We define $\underline{h}: \mathbf{R}^n \mathrm{x}\ \overset{\circ}{\mathbf{R}}_+^{n+1} \rightarrow \mathbf{R}^{2n}$ as :

$$h_i = \begin{cases} f_i(\underline{\alpha}, |\underline{V}|) - P_i^0 & i = 1,2,\ldots,n \\ |V_j|^{-1}(g_j(\underline{\alpha}, |\underline{V}|) + q_j(|V_j|)) & j = i-n;\ i = n+1,\ldots,2n \end{cases}$$

Similar to the classical representation, we partition $\underline{h}$ as $\underline{h}_1(\underline{\alpha}, |\underline{V}|): \mathbf{R}^n \mathrm{x} \overset{\circ}{\mathbf{R}}_+^{n+1} \rightarrow \mathbf{R}^{n+m}$ containing components 1 though n+m , and $\underline{h}_2(\underline{\alpha}, |\underline{V}|): \mathbf{R}^n \mathrm{x} \overset{\circ}{\mathbf{R}}_+^{n+1} \rightarrow \mathbf{R}^{n-m}$ containing components n+m+1 through 2n. The system equations are then given by:

$$\dot{\underline{\omega}} = -\mathbf{M}_g^{-1}\mathbf{D}_g\underline{\omega} - [\mathbf{M}_g^{-1}\mathbf{T}_1^T | 0]\, \underline{h}_1(\underline{\alpha}, |\underline{V}|) \tag{11a}$$
$$\dot{\underline{\alpha}} = \mathbf{T}_1\underline{\omega} - [\mathbf{T}_2\mathbf{D}_l^{-1}\mathbf{T}_2^T | 0]\, \underline{h}_1(\underline{\alpha}, |\underline{V}|) \tag{11b}$$
$$|\dot{\underline{V}}_1| = -[0 | \mathbf{D}_x]\, \underline{h}_1(\underline{\alpha}, |\underline{V}|) \tag{11c}$$
$$\underline{0} = \underline{h}_2(\underline{\alpha}, |\underline{V}|) \tag{11d}$$

where $\mathbf{M}_g, \mathbf{D}_g, \mathbf{D}_l$, and $\mathbf{T}$ are as defined in 3.1, and

$$\mathbf{D}_x = diag\left[\frac{x_{d,0} - x'_{d,0}}{T'_{d0,0}}, \frac{x_{d,1} - x'_{d,1}}{T'_{d0,1}}, \ldots, \frac{x_{d,m-1} - x'_{d,m-1}}{T'_{d0,m-1}}\right]$$

4. Drawbacks of Degenerate System Model

A mixed system of differential and algebraic constraints such as (10) or (11) is not guaranteed to define a globally well posed dynamical system. Specifically, we will show that for a very simple example of the power system model described by (10), "impasse point" behavior [6] occurs.

One may interpret the effects of the constraints in (10c) or (11d) from either an algebraic or geometric perspective. Algebraically, we view (10c) as implicitly defining $|\underline{V}|$ as a function of $\underline{\alpha}$. Roughly speaking, the implicit function theorem guarantees the existance of a local solution for $|\underline{V}|$ as a function of $\underline{\alpha}$ about any point $(\underline{\alpha}, |\underline{V}|)$ satisfying $\underline{h}_2(\underline{\alpha}, |\underline{V}|) = \underline{0}$ and $\frac{\partial \underline{h}_2}{\partial |\underline{V}_2|}(\underline{\alpha}, |\underline{V}|)$ nonsingular. One may then substitute the solution for $|\underline{V}|$ into (10a) and (10b) to obtain a local system of differential equations in $\underline{\omega}$ and $\underline{\alpha}$ alone. Variations of this approach provide the underlying theory for most power system simulation programs [19].

The geometric perspective, while less useful from a computational standpoint, offers insight into those cases where this process breaks down. Consider (10c) as defining a constraint manifold in the $\underline{\omega}, \underline{\alpha}, |\underline{V}|$ space. Trajectories of the system must remain on this manifold. Furthermore, the velocity vector which is tangent to the trajectory at any point must have the property that its $\dot{\underline{\omega}}$ and $\dot{\underline{\alpha}}$ components are given by (10a) and (10b). In [17], this process is described as "lifting" the dynamics onto the constraint manifold. We illustrate this process, and the potential for impasse point behavior, with the following simple example.

4.1. Example System

We consider a simple one machine example with the classical model, as shown in figure 1. The system is assumed to have a load located at the generator terminal bus, having frequency dependent real power demand and fixed reactive power demand. System equations (10) applied to this example yield:

$$\dot{\omega} = -M_g^{-1}D_g\omega + M_g^{-1}(P^0 - B_{01}|V_1|\sin\alpha) \quad (12a)$$

$$\dot{\alpha} = -D_l^{-1}(P^0 - B_{01}|V_1|\sin\alpha) - \omega \quad (12b)$$

$$0 = |V_1|^{-1}(-Q_1{}^0 - B_{01}|V_1|\cos\alpha - B_{11}|V_1|^2) \quad (12c)$$

For our example, we will take parameter values of:

$M_g = 10.0$

$D_g = 0.05$

$D_l = 0.05$

$B_{12} = -B_{11} = 10.0$

$Q_1{}^0 = -0.5$

$P^0 = -4.0$

Figure 2 shows the locus of points in the α versus $|V_1|$ plane satisfying (12c). Note that (12c) is independent of ω, so we may view the closed curve in figure 2 as the cross section of a tube of infinite extent in the ω direction. Superimposed on this is the curve of $h_1(\alpha, |V_1|) = B_{12}|V_1|\sin\alpha - P^0 = 0$. For $\omega=0$, this $h_1=0$ curve divides the plane into two regions: below the curve, $\dot{\alpha}$ is greater than zero, above the curve $\dot{\alpha}$ is less than zero. The effect of nonzero ω will be to shift this curve. However, given $D_l^{-1}=20.0$ in our example, this effect will be neglible. Therefore, for initial conditions of $\omega=0.0, \alpha=60°, |V_1| = 0.4$, the path of the resultant trajectory will be roughly as shown in figure 3. We see that the trajectory reaches $(\alpha^i, |V_1^i|)$ in finite time t^i (because $\dot{\alpha}$ is positive and bounded away from zero along the path shown) , but cannot be continued on the time interval $[0, t^i+\beta]$ for any $\beta>0$. As defined in [6], $(\alpha^i, |V_1^i|)$ is an impasse point.

While this example concentrated on the degenerate system given by (10) under the assumption of constant reactive load, it is easily shown that impasse point behavior can appear in more general power system examples.

4.2. Interpretation of Impasse Point Behavior

The appearance of nonphysical behavior such as impasse points suggests that our model is not applicable over the entire range of possible voltage magnitude variation. This conclusion is supported by the experience in simulation programs using fixed P-Q load models, where for low values of $|V_i|$ the process of solving for voltage magnitude as a function of angle may break down [11]. In simulation studies, a proposed solution is to instantaneously "switch" to a fixed impedance load at some threshold of voltage magnitude. Such an approach seems ill-advised in analytic studies without further evidence that it accurately reflects actual load behavior.

The alternative is to accept the degenerate model D as accurately reflecting load behavior in a limited range of values of the system variables. Field tests of loads suggest that this is true in a region about the steady state operating point. Our goal is to identify a region in which D remains well posed, and to restrict our region of attraction estimate to a subset of this region. The theory of singular perturbations provides a means to do this. We define an augmented (singularly perturbed) system, A_ε , which is well posed globally. We then find conditions which ensure that trajectories of the degenerate system can be approximated arbitrarily closely by the well behaved trajectories of the augmented system. Our region of attraction estimate is restricted to a set (which is shown to be invariant with respect to both D and A_ε) in which these conditions hold.

5. Augmented System Equations

Following the approach suggested in [17], we view (10c) and (11d) as the degenerate limit as $\varepsilon \to 0^+$ of :

$$\varepsilon |\dot{\underline{V}}_2| = -\underline{h}_2(\underline{\alpha}, |\underline{V}|) \tag{13}$$

The augmented system, which we denote A_ε , is then described by a set of autonomous differential equations. Again, we examine the two cases of classical and flux decay generator representations.

Case 1: Classical Model

$$\dot{\underline{\omega}} = -\mathbf{M}_g^{-1}\mathbf{D}_g\underline{\omega} - \mathbf{M}_g^{-1}\mathbf{T}_1{}^T\underline{h}_1(\underline{\alpha}, |\underline{V}|) \tag{14a}$$

$$\dot{\underline{\alpha}} = \mathbf{T}_1\underline{\omega} - \mathbf{T}_2\mathbf{D}_l^{-1}\mathbf{T}_2{}^T\underline{h}_1(\underline{\alpha}, |\underline{V}|) \tag{14b}$$

$$|\dot{\underline{V}}_2| = -\frac{1}{\varepsilon}\underline{h}_2(\underline{\alpha}, |\underline{V}|) \tag{14c}$$

Case 2: Flux Decay Model

$$\dot{\underline{\omega}} = -\mathbf{M}_g^{-1}\mathbf{D}_g\underline{\omega} - [\mathbf{M}_g^{-1}\mathbf{T}_1{}^T | 0]\underline{h}_1(\underline{\alpha}, |\underline{V}|) \tag{15a}$$

$$\dot{\underline{\alpha}} = \mathbf{T}_1\underline{\omega} - [\mathbf{T}_2\mathbf{D}_l^{-1}\mathbf{T}_2{}^T | 0]\underline{h}_1(\underline{\alpha}, |\underline{V}|) \tag{15b}$$

$$|\dot{\underline{V}}_1| = -[0 | \mathbf{D}_x]\underline{h}_1(\underline{\alpha}, |\underline{V}|) \tag{15c}$$

$$|\dot{\underline{V}}_2| = -\frac{1}{\varepsilon}\underline{h}_2(\underline{\alpha}, |\underline{V}|) \tag{15d}$$

By construction, it is clear that in the respective generator representations, the equilibria of D coincide with those of A_ε . A sufficient condition for a stable equilibrium of D to be stable with respect to A_ε is examined in section 7, after the machinery of a Lyapunov function for A_ε is developed.

6. Lyapunov Function for Augmented System

To define a Lyapunov function for the augmented system A_ε , we assume that the desired post fault operating point $\underline{x}^e$ has been identified. The candidate Lyapunov function will be defined relative to this point so that its value at $\underline{x}^e$ is zero. We will denote our candidate Lyapunov function $\mathbf{V}(\underline{x})$, with the dependence on $\underline{x}^e$ understood. In turn $\mathbf{V}(\underline{x})$ will be used to verify the asymptotic stability of $\underline{x}^e$.

Define:

$$\mathbf{V}(\underline{x}) = \tfrac{1}{2}\underline{\omega}^T\mathbf{M}_g\underline{\omega} + \int_{(\underline{\alpha}^e, |\underline{V}|^e)}^{(\underline{\alpha}, |\underline{V}|)} \langle \underline{h}(\underline{y}), d\underline{y} \rangle \tag{16}$$

A closed form equivalent for (16) is presented in Appendix A.

We have expressed (16) with the assumption that the integral term may be written independent of any C^1 path in $R^n x \overset{o}{R}_+^{n-m+1}$ (alternately $R^n x \overset{o}{R}_+^{n+1}$ for the flux decay model) . This follows directly from the observation that the Jacobean matrix:

$$J(\underline{\alpha}, |\underline{V}|) = \frac{d\underline{h}(\underline{y})}{d\underline{y}} \tag{17}$$

where $\underline{y} = \begin{bmatrix} \underline{\alpha} \\ |\underline{V}| \end{bmatrix}$, is symmetric. This calculation is performed in appendix A.

Next we must show that the derivative of $V(\underline{x})$ along trajectories of (14) or (15) is nonpositive. By direct calculation we obtain:

$$\dot{V}(\underline{x}) = -\underline{\omega}^T D_g \underline{\omega} - \underline{h}_1(\underline{\alpha}, |\underline{V}|)^T R \underline{h}_1(\underline{\alpha}, |\underline{V}|) - \frac{1}{\varepsilon} \underline{h}_2(\underline{\alpha}, |\underline{V}|)^T \underline{h}_2(\underline{\alpha}, |\underline{V}|) \tag{18}$$

where

$$R = \begin{cases} T_2 D_l^{-1} T_2^T & \text{for classical model} \\ \begin{bmatrix} T_2 D_l^{-1} T_2^T & 0 \\ 0 & D_x \end{bmatrix} & \text{for flux decay model} \end{cases}$$

By construction, D_g is positive definite and R is positive semi-definite. Hence $\dot{V}(\underline{x}) \le 0$.

Next, we use $V(\underline{x})$ to establish sufficient conditions for $\underline{x}^e$ to be asymptotically stable.

Proposition 6.1

Given an equilibrium point $\underline{x}^e$ with components $\underline{\omega}^e = \underline{0}$, $\underline{\alpha}^e$, and $|\underline{V}^e|$, if the matrix $J(\underline{\alpha}^e, |\underline{V}^e|)$ is positive definite, then $\underline{x}^e$ is asymptotically stable with respect to A_ε .

Proof:

First observe that the structure of (14) and (15) imply that $\underline{h}_1(\underline{\alpha}^e, |\underline{V}^e|) = \underline{0}$ and $\underline{h}_2(\underline{\alpha}^e, |\underline{V}^e|) = \underline{0}$. Hence $\frac{\partial V}{\partial \underline{x}} = \underline{0}$, and a Taylor expansion of $V(\underline{x})$ about $\underline{x}^e$ yields:

$$V(\underline{x}) = (\underline{x} - \underline{x}^e)^T \begin{bmatrix} M_g & 0 \\ 0 & J(\underline{\alpha}^e, |\underline{V}^e|) \end{bmatrix} (\underline{x} - \underline{x}^e) + o(||\underline{x} - \underline{x}^e||^3) \tag{19}$$

where $o(\cdot)$ represents higher order terms. Given $M_g > 0$ by construction, and the hypothesis $J(\underline{\alpha}^e, |\underline{V}^e|) > 0$, we have that $V(\underline{x}^e + \underline{x})$ is locally positive definite. We define:

$$S_k = \text{component of } \{\underline{x} \mid V(\underline{x}) \le k\} \text{ containing } \underline{x}^e \tag{20}$$

It is clear from (22) that for some $\bar{k}$ sufficiently small, $S_{\bar{k}}$ is bounded. Let

$$\Omega_0 = \{\underline{x} \mid \dot{V}(\underline{x}) = 0\} \tag{21}$$

Then it is easily shown that the largest invariant set of A_ε contained in $\Omega_0 \cap S_{\bar{k}}$ is the point $\underline{x}^e$. It follows from La Salle's theorem [21] that $\underline{x}^e$ is an asymptotically stable equilibrium for A_ε . ▪

7. Relation of Augmented System to Degenerate System

Our first step is to return to the issue raised in section 5; namely, under what conditions is a stable equilibrium $\underline{x}^e$ of D also stable with respect to A_ε.

Proposition 7.1

Suppose the equilibrium point $\underline{x}^e$ is "small disturbance stable" [23] with respect to D and $\frac{\partial \underline{h}_2}{\partial |\underline{V}_2|}(\underline{\alpha}^e, |\underline{V}^e|)$ is positive definite. Then $\underline{x}^e$ is asymptotically stable with respect to A_ε.

Proof:

To allow uniform notation for both the classical and flux decay representations, we will partition a subset of the system variables for each case into what we will refer to as dynamic and algebraic variables.

Case 1: Classical Model

$\underline{y}$ = vector of dynamic variables $= \underline{\alpha}$

$\underline{z}$ = vector of algebraic variables $= |\underline{V}|$

Case 2: Flux Decay Model

$\underline{y}$ = vector of dynamic variables $= \begin{bmatrix} \underline{\alpha} \\ |\underline{V}_1| \end{bmatrix}$

$\underline{z}$ = vector of algebraic variables $= |\underline{V}_2|$

By a minor variation on theorem 1 of [23], we have that $\underline{x}^e$ is small disturbance stable implies that

$$H(\underline{y}^e, \underline{z}^e) = \left\{ \frac{\partial \underline{h}_1}{\partial \underline{y}} - \frac{\partial \underline{h}_1}{\partial \underline{z}} \left[\frac{\partial \underline{h}_2}{\partial \underline{z}} \right]^{-1} \frac{\partial \underline{h}_2}{\partial \underline{y}} \right\}_{(\underline{y}^e, \underline{z}^e)} \tag{22}$$

is positive definite. By the definitions of $\underline{h}_2$ and $\underline{z}$, the second hypothesis of proposition 7.1 translates to $\frac{\partial \underline{h}_2}{\partial \underline{z}}(\underline{y}^e, \underline{z}^e) > 0$. Using the results of proposition 6.1, we must show that $H(\underline{y}^e, \underline{z}^e) > 0$ and $\frac{\partial \underline{h}_2}{\partial \underline{z}}(\underline{y}^e, \underline{z}^e) > 0$ imply that $J(\underline{\alpha}^e, |\underline{V}^e|) > 0$. This follows directly from the observation that [18]:

$$[\underline{y}^T | \underline{z}^T] J(\underline{\alpha}^e, |\underline{V}^e|) \begin{bmatrix} \underline{y} \\ \underline{z} \end{bmatrix} = \underline{y}^T H(\underline{y}^e, \underline{z}^e) \underline{y}$$
$$+ \left\| \left[\frac{\partial \underline{h}_2}{\partial \underline{z}}(\underline{y}^e, \underline{z}^e) \right]^{-1/2} \left[\frac{\partial \underline{h}_2}{\partial \underline{y}}(\underline{y}^e, \underline{z}^e) \right] \underline{y} + \left[\frac{\partial \underline{h}_2}{\partial \underline{z}}(\underline{y}^e, \underline{z}^e) \right]^{1/2} \underline{z} \right\|^2$$

To put the results of propositions 7.1 and 7.2 into perspective, we envision the following application. One is given a desired post fault operating point $\underline{x}^e$ for D, which is small disturbance stable (this is a reasonable minimal stability requirement for any operating point). To ensure that this point is also asymptotically stable with respect to A_ε, we must also check that $\frac{\partial \underline{h}_2}{\partial \underline{z}} > 0$. Simple sufficiency conditions for this property are examined in appendix A.

7.1. Region of Attraction Estimate for Augmented System A_ε

In proposition 6.1, we established that $\underline{x}^e$ was an asymptotically stable equilibrium of A_ε by invoking LaSalle's theorem for the set S_ξ. The conclusion was that any trajectory originating in $S_{\bar{k}}$ converged to $\underline{x}^e$ as $t \to \infty$. In addition to providing the asymptotic stability result, this implies by definition that $S_{\bar{k}}$ is contained in the region of attraction of $\underline{x}^e$. The goal of this section is to show that as the parameter k is increased, the sets S_k remain in the region of attraction of $\underline{x}^e$ until some critical value, k_{crit}, is reached. This limiting value of k is obtained when the set S_k fails to be bounded. We address sufficient conditions for boundedness in the following proposition.

Proposition 7.2

Define

$$S_k / S_{\bar{k}} = \{ \underline{x} \,|\, \underline{x} \in S_k, \underline{x} \notin S_{\bar{k}} \}$$

Note that for $k \le \bar{k}$, $S_k / S_{\bar{k}} = \phi$. Suppose that for some $k > \bar{k}$

$$\inf_{\underline{x} \in S_k / S_{\bar{k}}} ||\nabla V(\underline{x})|| > 0$$

Then the set S_k is bounded and $V(\underline{x}) \ge 0$ for all $\underline{x} \in S_k$.

Proof

A detailed proof of this proposition will be given in appendix B; here we will simply contrast the result with that generally used in Lyapunov studies for power systems. In [22] for example, the constant potential surface (here the boundary of S_k) is expanded until it first intersects an unstable equilibrium point. The value of $V(\underline{x})$ at this point is taken as the desired k_{crit}, and for all $k < k_{crit}$, S_k is claimed to lie in the region of attraction of $\underline{x}^e$. Implicit in this approach is the assumption that S_k remain bounded until the closest unstable equilibrium point is encountered, otherwise LaSalle's theorem does not hold. For the Lyapunov function defined in (16), this boundedness assumption may not hold for an arbitrary network. Hence the more complex criterion for boundedness proposed in proposition 7.2 is necessary.

For the Lyapunov function defined here, we will define the smallest k for which the hypothesis of 7.2 fails to hold k_{crit}. With boundedness established for S_k, $0 < k < k_{crit}$, we may obtain an estimate of the region of attraction of $\underline{x}^e$.

Proposition 7.3

Let the assumptions on k of propositin 7.2 hold. Then S_k is invariant with respect to A_ε, and S_k is contained in the region of attraction of $\underline{x}^e$ for A_ε.

Proof

The invariance of S_k follows from the fact that $\dot{V}(\underline{x}) \le 0$ and the construction of S_k. To show that any trajectory of A_ε originating in S_k approaches $\underline{x}^e$ as $t \to \infty$, we apply LaSalle's theorem as in proposition 6.1 ▪.

It is important to note that several researchers [3,9,15] have obtained excellent results in applications using heuristic techniques for finding k_{crit}, which have reduced the conservativeness of the region of attraction estimates used in their studies. Presumably such heuristic techniques might be profitably applied to the Lyapunov function and models proposed here. However, no formal proof has been offered to show that the larger sets obtained by these methods must lie inside the true region of attraction.

7.2. Region of Attraction Estimate for Degenerate System D

We recall that our original, physically based model is the degenerate system, D. As observed in section 4, D is not necessarily well posed globally. Therefore, within the limitations of this model the region of attraction estimate should have the property that any trajectory originating in this set is well defined for all time (no impasse point behavior), and asymptotically approaches the stable equilibrium $\underline{x}^s$. We will use the sets S_k defined previously, suitably restricting k so that the desired properties are obtained.

Proposition 7.4

Let the assumptions of proposition 7.1 hold. Then for all k, $0<k<k_{crit}$ such that

$$\inf_{\underline{x}\in S_k} \lambda_{\min}\left[\frac{\partial \underline{h}_2}{\partial \underline{z}}(\underline{x})\right]>0 \tag{23}$$

(where $\lambda_{\min}[A]$ denotes the smallest eigenvalue of the matrix $\mathbf{A}$), any trajectory $s_0(t,\underline{x}^0)$ of D with initial condition $\underline{x}^0 \in S_k$ has the following properties:

(i) $s_0(t,\underline{x}^0) \in S_k$ for all $t\geq 0$ (i.e. S_k is invariant with respect to D)

(ii) for all $\delta>0$, there exists $\varepsilon>0$ such that the trajectory of A_ε with initial condition $\underline{x}^0$, denoted $s_\varepsilon(t,\underline{x}^0)$ satisfies $||s_0(t,\underline{x}^0)-s_\varepsilon(t,\underline{x}^0)||\leq\delta$ for all $t\geq 0$.

(iii) $s_0(t,\underline{x}^0)\to\underline{x}^s$ as $t\to\infty$

Proof

Property (i)

Our condition on the smallest eigenvalue of $\frac{\partial \underline{h}_2}{\partial \underline{z}}(\underline{x})$ over the set S_k guarantees that there exists an $\overline{M}$ such that $||[\frac{\partial \underline{h}_2}{\partial \underline{z}}(\underline{x})]^{-1}||_2\leq\overline{M}$ for all $\underline{x} \in S_k$, and in particular for $\underline{x}^0$. By the implicit function theorem [16], we have that $\frac{\partial \underline{h}_2}{\partial \underline{z}}(\overline{\underline{x}})$ nonsingular implies that there exist open balls U and V about $\overline{\underline{y}}$ and $\overline{\underline{z}}$ respectively and a unique C^∞ (by virtue of $\underline{h}_2$ being C^∞) function $\varphi: U\to V$ such that $\underline{h}_2(\underline{y},\underline{\varphi}(\underline{y})) = \underline{0}$ for all $\underline{y} \in U$. Moreover, given the fixed upper bound on $||[\frac{\partial \underline{h}_2}{\partial \underline{z}}]^{-1}||_2$ over S_k, we can find a minimum $r>0$ so that all such balls U have radius of at least r. Hence we may form a finite cover of the $\underline{y}$ components of the bounded set S_k by these open balls, which we denote $\{U_r(\underline{y}^i)\}$. Starting from $\underline{x}^0 \in S_k$, we obtain a local representation of D on $U_r(\underline{y}^0)$ by:

$$\dot{\underline{\omega}} = -\mathbf{M}_g^{-1}\mathbf{D}_g\underline{\omega} - \mathbf{A}\underline{h}_1(\underline{y},\underline{\varphi}(\underline{y})) \tag{24a}$$

$$\dot{\underline{y}} = \mathbf{B}\underline{\omega} - \mathbf{C}\underline{h}_1(\underline{y},\underline{\varphi}(\underline{y})) \tag{24b}$$

where $\mathbf{A}$, $\mathbf{B}$, and $\mathbf{C}$ are constant real matrices dependent on the generator representation chosen.

Using $\underline{\varphi}$, we may also express the Lyapunov function defined in (16) as

$$\mathbf{V}(\underline{\omega},\underline{y}) = \mathbf{V}(\underline{\omega},\underline{y},\underline{\varphi}(\underline{y})) \tag{25}$$

Along trajectories of (24) we have:

$$\dot{\mathbf{V}}(\underline{\omega},\underline{y}) = -\underline{\omega}^T\mathbf{D}_g\underline{\omega} - \underline{h}_1^T(\underline{y},\underline{\varphi}(\underline{y}))\,\mathbf{R}\underline{h}_1(\underline{y},\underline{\varphi}(\underline{y})) -$$

$$\underline{h}_2^T(\underline{y},\underline{\varphi}(\underline{y}))\left[\frac{\partial h_2}{\partial \underline{z}}(\underline{y},\underline{\varphi}(\underline{y}))\right]^{-1}\left[\frac{\partial h_2}{\partial \underline{y}}(\underline{y},\underline{\varphi}(\underline{y}))\right]\underline{h}_1(\underline{y},\underline{\varphi}(\underline{y})) \quad (26)$$

where **R** is a positive semidefinite matrix dependent on the generator representation used, and by definition $\underline{h}_2(\underline{y},\underline{\varphi}(\underline{y})) = \underline{0}$. Hence $\dot{V}(\underline{\omega},\underline{y}) \le 0$.

Because $\dot{V}(\underline{\omega},\underline{y}) \le 0$, we conclude that the $\underline{y}$ component of trajectory $s_0(t,\underline{x}^0)$ for the local representation of D remains in $U_r(\underline{y}^0) \cap S_k$ on some finite time interval $[0,t^1)$. When $s_0(t,\underline{x}^0)$ leaves $U_r(\underline{y}^0)$ at time t^1, we must switch to a new local representation corresponding to the ball in which $s_0(t^1,\underline{x}^0)$ lies, say $U_r(\underline{y}^1)$. The same reasoning shows that $s_0(t,\underline{x}^0)$ remains in $U_r(\underline{y}^1) \cap S_k$ on some interval $[t^1,t^2)$. Given that the right hand side of (24) remains bounded and Lipschitz continuous in S_k, standard continuation results for o.d.e.'s ensure that $s_0(t,\underline{x}^0)$ can be continued for all $t \ge 0$, and by $\dot{V}(\underline{\omega},\underline{y}) \le 0$ we have that these trajectories remain in S_k. ▪ (propertry (i))

To establish properties (ii) and (iii), we will make use of the following lemma:

Lemma 7.4.1 :

Given $\underline{x}^0 \in S_k$, for all $\bar{k}>0$, there exists $\bar{\varepsilon}>0$ and an $T<\infty$ such that $s_\varepsilon(T,\underline{x}^0) \in S_{\bar{k}}$ for all ε, $0<\varepsilon\le\bar{\varepsilon}$.

A detailed proof of this lemma is provided in appendix B. A brief motivation is in order, however. In proposition 6.1, we established that for fixed ε, $\underline{x}^0 \in S_k$ implied that $s_\varepsilon(t,\underline{x}^0) \to \underline{x}^s$ as $t \to \infty$. This of course implies that for an arbitrary $\bar{k}>0$, $s_\varepsilon(t,\underline{x}^0)$ will eventually enter $S_{\bar{k}}$. Lemma 7.4.1 goes further by establishing a type of uniform stability in ε. Specifically, we show that given any $\bar{k}>0$ (presumably $\bar{k} \ll k$), we can find an $\bar{\varepsilon}$ and a T such that not only is $s_{\bar{\varepsilon}}(T,\underline{x}^0)$ in $S_{\bar{k}}$, but $s_\varepsilon(T,\underline{x}^0)$ is in $S_{\bar{k}}$ for all $0<\varepsilon\le\bar{\varepsilon}$. With this property established, we can easily show properties (ii) and (iii) using singular perturbation results.

Properties (ii) and (iii)

If we examine the augmented equations (14) and (15) in light of the notation developed in section 7, we see that the perturbed equations of (14c) and (15d) become:

$$\dot{\underline{z}} = -\frac{1}{\varepsilon}\underline{h}_2(\underline{y},\underline{z}) \quad (27)$$

Then condition (23) and point (i) insure that when (27) is linearized about any point on $s_0(t,\underline{x}^0)$, all its eigenvalues have strictly negative real parts. Hence by the results of [13] we have that for all $T<\infty$, and all $\delta>0$, there exists a $\bar{\varepsilon}>0$ such that $0<\varepsilon\le\bar{\varepsilon}$ implies $||s_0(t,\underline{x}^0)-s_\varepsilon(t,\underline{x}^0)||\le\delta$ for all $t \in [0,T]$.

Next we observe that by the construction of the sets S_k, given any $\delta>0$, there exists k^1, $k^2>0$ and $\bar{\delta}>0$ such that

(a) $S_{k^2} \subset B(\underline{x}^s,\delta) = \{\underline{x} \mid ||\underline{x}-\underline{x}^s|| \le \delta\}$

(b) $B(\underline{x}^s,\bar{\delta}) \subset S_{k^2}$, and $S_{k^1} \subset B(\underline{x}^s,\frac{\bar{\delta}}{2})$

The nesting of sets described in points (a) and (b) is described in figure 4. By the results of lemma 7.4.1, we may find ε^1 and T^1 such that $s_\varepsilon(T^1,\underline{x}^0)) \in S_{k^1}$ for all ε satisfying $0<\varepsilon\le\varepsilon^1$. By the result of [13] used above, we may find an $\varepsilon^2>0$ such that $0<\varepsilon\le\varepsilon^2$ implies $||s_0(t,\underline{x}^0)-s_\varepsilon(t,\underline{x}^0)||\le\frac{\bar{\delta}}{2}$ for all $t \in [0,T^1]$. If we let $\bar{\varepsilon}$

$= \min(\varepsilon^1, \varepsilon^2)$, we have $0<\varepsilon\leq\bar{\varepsilon}$ implies :

(a) $||s_0(t,\underline{x}^0)-s_\varepsilon(t,\underline{x}^0)|| \leq \frac{\bar{\delta}}{2} < \delta$ for all $t \in [0,T^1]$

(b) $s_\varepsilon(t,\underline{x}^0) \in S_{k^1} \subset B(\underline{x}^0, \frac{\bar{\delta}}{2})$ for all $t \geq T^1$.

Results (a) and (b) together imply that $s_0(T^1,\underline{x}^0) \in B(\underline{x}^0,\bar{\delta}) \subset S_{k^2} \subset B(\underline{x}^0,\delta)$ which in turn implies that $||s_0(t,\underline{x}^0)-s_\varepsilon(t,\underline{x}^0)|| \leq \delta$ for all $t \geq 0$. Properties (ii) and (iii) follow directly. ▪

Proposition 7.4 provides a means of identifying those values of k for which the sets S_k are suitable region of attraction estimates for D . While the criterion of the smallest eigenvalue of $\frac{\partial \underline{h}_2}{\partial \underline{z}} > 0$ over the set S_k may be computationally unwieldly, the fact that $\frac{\partial \underline{h}_2}{\partial \underline{z}}$ is a real symmetric matrix offers an easy sufficiency condition for this property. This issue is examined in appendix A.

8. Conclusions

In this work we have examined a detailed model for direct transient stability analysis of multimachine power systems. We have shown that this model is not generally well posed globally. To address the problem, we have used singular perturbation techniques to introduce an augmented system which is globally well posed, and first performed stability analysis for the augmented system. In the process a valid Lyapunov function for the augmented system is constructed. Finally, we have obtained explicit criteria for the trajectories of the augmented system to "behave like" those of the original system , and have shown that a region of attraction estimate may be found in which these criteria are met.

It should be pointed out that the augmented system and singular perturbation results are primarily conceptual tools for identifying the Lyapunov function, region of attraction estimates, and "valid" regions for the degenerate model. Similar results could be obtained by working directly with the degenerate model. However, we believe that the motivation is much clearer in the context presented here. In particular, the concept and construction of a Lyapunov function is not well established when dealing with a system of differential equations with algebraic constraints. By working with the augmented system first, we may employ standard results from Lyapunov theory directly. The singualr perturbation results allow us to "translate" back to the original degenerate model.

Ultimately, through improved understanding of dynamic load behavior in power systems, one may hope to obtain a system model which is well posed globally, eliminating the necessity for these techniques. However, given the state of the art of power system modelling, the approach presented here represents a means of applying Lyapunov techniques to the degenerate power system model. More generally, it provides a means of obtaining region of attraction estimates for any system modelled by ordinary differential equations with algebraic constraints.

Appendix A

Structure of $J(\underline{\alpha}, |\underline{V}|)$

By definition

$$J = \begin{bmatrix} \dfrac{\partial \underline{f}}{\partial \underline{\alpha}} & \dfrac{\partial \underline{f}}{\partial |\underline{V}|} \\ \dfrac{\partial [\,|\mathbf{V}|\,]^{-1}(\underline{g}+\underline{q})}{\partial \underline{\alpha}} & \dfrac{\partial [\,|\mathbf{V}|\,]^{-1}(\underline{g}+\underline{q})}{\partial |\underline{V}|} \end{bmatrix} \tag{17}$$

where $[\,|\mathbf{V}|\,] = diag[\,|V_0|, |V_1|, \cdots, |V_n|\,]$.

To show J is symmetric, we must show:

(a) $\dfrac{\partial \underline{f}}{\partial \underline{\alpha}}$ symmetric

(b) $\dfrac{\partial [\,|\mathbf{V}|\,]^{-1}(\underline{g}+\underline{q})}{\partial |\underline{V}|}$ symmetric

(c) $\left[\dfrac{\partial [\,|\mathbf{V}|\,]^{-1}(\underline{g}+\underline{q})}{\partial \underline{\alpha}}\right]^T = \dfrac{\partial \underline{f}}{\partial |\underline{V}|}$

Point (a)

$$\frac{\partial f_i(\underline{\alpha}, |\underline{V}|)}{\partial \alpha_i} = \begin{cases} -B_{ij}\,|V_i|\,|V_j| \cos(\alpha_i - \alpha_j) & i \neq j \\ \sum_{\substack{k=0 \\ k \neq i}}^{n} B_{ik}\,|V_i|\,|V_k| \cos(\alpha_i - \alpha_k) & i = j \end{cases} \tag{A.1}$$

Given $B_{ij}\cos(\alpha_i - \alpha_j) = B_{ji}\cos(\alpha_j - \alpha_i)$ symmetry follows immediately.

Point (b)

$$\frac{\partial |V_i|^{-1}(g_i(\underline{\alpha}, |\underline{V}|) + q_i(|V_i|))}{\partial |V_j|} = \begin{cases} -B_{ij}\cos(\alpha_i - \alpha_j) & i \neq j \\ -B_{ii} + \dfrac{\partial(|V_i|^{-1} q_i(|V_i|))}{\partial |V_j|} & i = j \end{cases} \tag{A.2}$$

Symmetry follows as in point (a).

Point (c)

$$\frac{\partial(|V_i|^{-1}(g_i(\underline{\alpha}, |\underline{V}|) + q_i(|V_i|)))}{\partial \alpha_j} = \begin{cases} -B_{ij}\,|V_j| \sin(\alpha_i - \alpha_j) & i \neq j \\ \sum_{k=0}^{n} B_{ik}\,|V_k| \sin(\alpha_i - \alpha_k) & i = j \end{cases} \tag{A.3}$$

$$\frac{\partial f_i(\underline{\alpha}, |\underline{V}|)}{\partial |V_j|} = \begin{cases} B_{ij}\,|V_i| \sin(\alpha_i - \alpha_j) & i \neq j \\ \sum_{k=0}^{n} B_{ik}\,|V_k| \sin(\alpha_i - \alpha_k) & i = j \end{cases} \tag{A.4}$$

Sufficient Conditions for $\dfrac{\partial \underline{h}_2}{\partial \underline{z}}(\underline{y}^e, \underline{z}^e)$ Positive Definite

From the definition of $\underline{y}$, $\underline{z}$, $\underline{h}_2(\underline{y}, \underline{z})$ in section 7 and results above, it is clear that $\dfrac{\partial \underline{h}_2}{\partial \underline{z}}(\underline{y}^e, \underline{z}^e)$ is symmetric, with components given by (A.2). From the Gershgorin circle criterion, we obtain the following sufficient condition for positive definiteness in terms of component values:

$$\sum_{\substack{k=0 \\ k\neq i}}^{n} | B_{ik}\cos(\alpha_i^e-\alpha_k^e) | < \sum_{\substack{k=0 \\ k\neq i}}^{n} B_{ik} - \frac{d}{d|V_i|}\left\{\frac{q_i(|V_i|)}{|V_i|}\right\}_{|V_i|=|V_i^e|} \qquad \text{(A.5)}$$

for $i = m, m+1, \ldots, n$

Closed Form for Lyapunov Function $V(\underline{x})$

The following function may be shown to have the same derivative with respect to $\underline{x} = (\underline{\omega}, \underline{\alpha}, |\underline{V}|)$ as $V(\underline{x})$, and to be equal to $V(\underline{x}^e) = 0$ at the stable equilibrium $\underline{x}^e$. Therefore the functions are equal, and we may write:

$$V(\underline{x}) = \tfrac{1}{2}\underline{\omega}^T \mathbf{M}_g \underline{\omega} - \tfrac{1}{2}\sum_{i=0}^{n}\sum_{k=0}^{n} B_{ik} |V_i||V_k| \cos(\alpha_i - \alpha_k)$$

$$+ \tfrac{1}{2}\sum_{i=0}^{n}\sum_{k=0}^{n} B_{ik} |V_i^e||V_i^e| \cos(\alpha_i^e - \alpha_k^e)$$

$$+ \sum_{k=r}^{n} \int_{|V_k^e|}^{|V_k|} \frac{q_k(x)}{x} dx - \underline{P}^T(\underline{\alpha} - \underline{\alpha}^e) \qquad \text{(A.6)}$$

where $r=m$ for the classical model and $r=0$ for the flux decay model. A very similar "energy function" was proposed in [14] for the case of classical generator models. While (A.6) is obviously preferable from a computational standpoint, (16) greatly simplifies the necessary analysis to verify the Lyapunov function properties.

Derivation of Flux Decay Model

For simplicity, we neglect the effect of saliency on the "power-angle" relation. Therefore the power delivered to the network by generator i with terminal bus voltage magnitude $|V_j|$ is given by:

$$P = \frac{E_{q,i}'|V_j|}{x_{d,i}'}\sin(\alpha_i - \alpha_j) \qquad \text{(A.7)}$$

We will define the ficticious internal bus voltage magnitude for generator i as $|V_i| = E_q'$, and let $B_{ij} = \frac{1}{x_{d,i}'}$. Then (A.7) becomes

$$P = B_{ij}|V_i||V_j|\sin(\alpha_i - \alpha_j) \qquad \text{(A.8)}$$

which is consistant with (2).

Following the development in [2], we employ the "one-axis" model to describe the time rate of change of $E_{q,i}'$ as

$$\dot{E}_{q,i}' = \frac{1}{T_{d0,i}'}E^0_{f,i} - E_i \qquad \text{(A.9)}$$

where excitation $E^0_{f,i}$ is fixed in our model, and

$$E_i = E_{q,i}' - (x_{d,i} - x_{d,i}')I_{d,i} \qquad \text{(A.10)}$$

$$E_{q,i}' = V_{q,j} + rI_{q,i} + x_{d,i}'I_{d,i} \qquad \text{(A.11)}$$

Neglecting resistance r , we solve for $I_{d,i}$ in (A.11). Substituting for $I_{d,i}$ in (A.10) and for E_i in (A.9) yields

$$\dot{E}_{q,i} = \frac{1}{T_{d0,i}'}(E^0_{f,i} - E_{q,i}' - \frac{x_{d,i} - x_{d,i}'}{x_{d,i}'}(E'_{q,i} - V_{q,j})) \qquad \text{(A.12)}$$

The quantity $V_{q,j}$ represents the q-axis component of V_j , and by definition V_j has an angle of $(\alpha_i - \alpha_j)$ relative to the q axis. Hence we obtain

$$V_{q,j} = |V_j| \cos(\alpha_i - \alpha_j) \tag{A.13}$$

Recalling our definition of $|V_i| = E_{q,i}'$, we may substitute in (A.12) to obtain

$$|\dot{V}_i| = \frac{1}{T_{d0,i}'}\left[E^0{}_{f,i} - |V_i| - \frac{x_{d,i} - x_{d,i}'}{x_{d,i}'}(|V_i| - |V_j| \cos(\alpha_i - \alpha_j))\right] \tag{A.14}$$

as given in (7).

Appendix B

Proposition 7.2: Outline of Proof

We wish to show that for any k satisfying the premise of proposition 7.2, the set S_k is bounded. Our approach will be to construct a homeomorphism between the boundary of the bounded set $S_{\bar{k}}$ (denoted $\partial S_{\bar{k}}$) and the boundary of S_k (∂S_k). ——

Consider the autonomous system

$$\dot{\underline{x}} = \nabla V(\underline{x}) \tag{B.1}$$

By construction of $V(\underline{x})$, it is easily shown that in any closed bounded set, $\nabla V(\underline{x})$ is bounded and Lipschitz continuous. Also, $V(\underline{x})$ is clearly nondecreasing along trajectories of (B.1). We will use these properties to show that for all $\bar{\underline{x}} \in \partial S_{\bar{k}}$, the trajectory of (B.1) originating from $\bar{\underline{x}}$ moves outward from $\partial S_{\bar{k}}$ and reaches a bounded $\underline{x}_f(\bar{\underline{x}})$ satisfying $V(\underline{x}_f(\bar{\underline{x}})) = k$. The map $\underline{x}_f(\cdot)$ is the desired homeomorphism.

Detailed Proof

Denote solutions of (B.1) with initial condition $\underline{x}^0$ as $s_0(t,\underline{x}^0)$. By standard continuation results for differential equations [7], the properties of $\nabla V(\underline{x})$ guarantee that for there exists a $\gamma>0$ such that (B.1) has a unique C^1 solution $s(t,\bar{\underline{x}})$ for all $t \in [0,\gamma]$.

Lemma 7.2.1

We will show that for all $\bar{\underline{x}} \in \partial S_{\bar{k}}$ there exists $\bar{t}<\infty$ such that

(i) $s(t,\bar{\underline{x}})$ is C^1 and exists on the time interval $[0,\bar{t}]$.

(ii) $V(s(\bar{t},\bar{\underline{x}})) = k$

(iii) $0<V(s(t,\bar{\underline{x}}))<k$ for all $t \in [0,\bar{t})$

Case 1:

Suppose for all $\bar{\underline{x}} \in \partial S_{\bar{k}}$, $s(t,\bar{\underline{x}})$ is C^1 and uniquely defined on $[0,\infty)$, so (i) is satisfied for all $\bar{t}<\infty$. Approach (ii) by contradiction. Given that the map $t \to V(s(t,\bar{\underline{x}}))$ is continuous, and $V(s(0,\bar{\underline{x}})) = \bar{k}<k$, if we suppose (ii) does not hold for any $0<\bar{t}<\infty$, it follows that $V(s(t,\bar{\underline{x}}))<k$ for all $0<\bar{t}<\infty$, which implies

$$s(t,\bar{\underline{x}}) \in S_k / S_{\bar{k}} \tag{B.2}$$

for all $t \in [0,\infty)$.

Then by the premise of proposition 7.2 there exists $\delta>0$ such that $\|\nabla V(s(t,\bar{\underline{x}}))\|>\delta$ for all $t \in [0,\infty)$. It follows that

$$V(s(t,\bar{\underline{x}}))-\bar{k} = \int_0^t \frac{d}{d\tau}\{V(s(\tau,\bar{\underline{x}}))\}d\tau \tag{B.3}$$

$$= \int_0^t \|\nabla V(s(\tau,\bar{\underline{x}}))\|^2 d\tau \geq \delta^2 \cdot t$$

But clearly for t sufficiently large we have $V(s(t,\bar{\underline{x}}))>k$ which yields the desired contradiction. Hence (ii) is satisfied. It is easily shown that a minimum such t must exist, and by the continuity of $t \to V(s(t,\bar{\underline{x}}))$ (iii) is satisfied. ▪ (case 1)

Case 2:

Suppose for some $\underline{x} \in \partial S_{\underline{E}}$, (B.1) does have a unique C^1 solution on $[0,t_f)$, but this solution cannot be uniquely continued on any interval $[0,t_f+\beta]$, $\beta>0$. Hence (i) holds for any $0<t<t_f$. It follows that [7]

$$\lim_{t \to t_f^-} s(t,\underline{x})$$

is not contained in any region where $\nabla V(\cdot)$ is bounded and Lipschitz continuous.

We establish (ii) by contradiction. Suppose for all $t \in [0,t_f)$, $V(s(t,\underline{x}))<k$. Recall that $\frac{d}{dt}(s(t,\underline{x}))= \nabla V(s(t,\underline{x}))$. Using this fact we may bound $||s(t,\underline{x})||$ by $||\underline{x}||$ plus the arc length of $s(t,\underline{x})$ from 0 to t , which may be computed as:

$$||s(t,\underline{x})||_2 = ||\underline{x}||_2+\int_0^t < \frac{s(\tau,\underline{x})}{||s(\tau,\underline{x})||_2}, \nabla V(s(\tau,\underline{x}))>d\tau$$

$$\leq ||\underline{x}||_2+\int_0^t ||\nabla V(s(\tau,\underline{x}))||_2 d\tau$$

If we break the interval $[0,t]$ into the set of points for which $||\nabla V(s(t,\underline{x}))||\leq 1$ and those for which $||\nabla V(s(t,\underline{x}))||>1$, we have :

$$||s(t,\underline{x})||_2 \leq ||\underline{x}||_2+t+\int_0^t ||\nabla V(s\tau,\underline{x}))||_2^2 d\tau \leq ||\underline{x}||_2 + t_f + k \qquad \text{(B.4)}$$

for all $t \in [0,t_f)$.

Hence

$$\lim_{t \to t_f^-} ||s(t,\underline{x})||_2 \leq t_f + k + ||\underline{x}||_2$$

Here we must distinguish between the two types of reactive load representation defined in (5). For the exponential representation or the polynomial representation with $q_i^0=0$, the boundedness of $||s(t,\underline{x})||$ as $t \to t_f$ implies $\nabla V(s(t,\underline{x})))$ remains bounded and Lipschitz continuous as $t \to t_f$, which contradicts our observation at the start of case 2.

For the case of polynomial reactive load representations with $q_i^0<0$ (recall our restriction in equation (5)) , we have the possibility of components of $\nabla V(\underline{x})$ becoming unbounded as the corresponding component of $|\underline{V}|$ goes to zero . However, in this case $V(s(t,\underline{x}))$ approaches ∞^+ , (see (A.6)), so we obtain a contradiction to $V(s(t,\underline{x}))<k$ for all $t \in [0,t_f)$.

We conclude that for either load representation (ii) must hold for some $\bar{t}<t_f$. Point (iii) follows from the same arguments employed for case 1. ▪ (lemma 7.2.1)

With lemma 7.2.1 established, we may define a function $\tau_k(\cdot):\partial S_{\underline{E}} \to R_+$, k satisfying the premise of proposition 7.2:

$$\tau_k(\underline{x}) = \text{smallest } t>0 \text{ such that } V(s(t,\underline{x}))=k$$

We will show that $\tau_k(\cdot)$ is continuous, and therefore that $x_f(\cdot) = s(\tau_k(\cdot),\cdot)$ is continuous .

Given $\underline{x} \in \partial S_{\underline{E}}$ and $\varepsilon>0$, let $\underline{x}' \in \partial S_{\underline{E}}$ satisfy $||\underline{x}-\underline{x}'||<\varepsilon$. Without loss of generality, we may assume $\tau_k(\underline{x})\leq\tau_k(\underline{x}')$ and let $T_{\min} = \tau_k(\underline{x})$. Then by continuity of $s(t,\cdot)$ with respect to initial conditions and continuity of $\nabla V(\cdot)$, for any $\delta_1>0$, there exists an appropriate ε such that the assumption of $||\underline{x}-\underline{x}'||<\varepsilon$

implies

$$\left| \| \nabla V(s(\zeta,\underline{x})) \|^2 - \| \nabla V(s(\zeta,\underline{x}')) \|^2 \right| < \delta_1$$

for all $\zeta \in [0, T_{\min}]$.

This implies

$$\int_0^{T_{\min}} \left\{ \| \nabla V(s(\zeta,\underline{x})) \|^2 - \| \nabla V(s(\zeta,\underline{x}')) \|^2 \right\} d\zeta \leq \delta_1 \cdot T_{\min}$$

But

$$\int_0^{T_{\min}} \| \nabla V(s(\zeta,\underline{x})) \|^2 d\zeta = k - \bar{k}$$

and

$$k - \bar{k} = \int_0^{\tau_k(\underline{x}')} \| \nabla V(s(\zeta,\underline{x}')) \|^2 d\zeta$$

$$= \int_0^{T_{\min}} \| \nabla V(s(\zeta,\underline{x}')) \|^2 d\zeta + \int_{T_{\min}}^{\tau_k(\underline{x}')} \| \nabla V(s(\zeta,\underline{x}')) \|^2 d\zeta$$

which implies that

$$\int_{T_{\min}}^{\tau_k(\underline{x}')} \| \nabla V(s(\zeta,\underline{x}')) \|^2 d\zeta \leq \delta_1 \cdot T_{\min}$$

By the definition of $\tau_k(\cdot)$, we have $s(\zeta,\underline{x}') \in S_k$ for all $\zeta \in [T_{\min}, \tau_k(\underline{x}')]$. Therefore $\| \nabla V(s(\zeta,\underline{x}')) \|^2 \geq \delta^2$ for all $\zeta \in [T_{\min}, \tau_k(\underline{x}')]$, where δ is as described in (B.3).

We conclude that

$$\delta_1 \cdot T_{\min} \geq \int_{T_{\min}}^{\tau_k} (\underline{x}') \| \nabla V(s(\zeta,\underline{x}')) \|^2 d\zeta$$

$$\geq \delta^2 | \tau_k(\underline{x}') - T_{\min} | = \delta^2 | \tau_k(\underline{x}') - \tau_k(\underline{x}) |$$

By construction $T_{\min} \leq \frac{k}{\delta^2}$, so it follows that

$$| \tau_k(\underline{x}') - \tau_k(\underline{x}) | \leq \frac{k}{\delta^2} \delta_1$$

for all $\underline{x}'$ such that $\| \underline{x}' - \underline{x} \| \leq \varepsilon$. Hence $\tau_k(\cdot)$ is continuous on $\partial S_{\bar{k}}$.

As indicated previously, we then have $x_f(\cdot)$: $\partial S_{\bar{k}} \to \partial S_k$ continous by observing $x_f(\underline{x}) = s(\tau_k(\underline{x}), \underline{x})$. To show that the inverse of $x_f(\cdot)$ is continuous, we need only observe that it is obtained by running the system (B.1) backwards in time from points on ∂S_k and repeating the preceeding construction. That $x_f(\cdot)$ is one to one follows from the uniqueness of the solutions of the differential equation (B.1). Finally, to show that $x_f(\partial S_{\bar{k}}) = \partial S_k$, it is easily established that for all $\underline{x} \in \partial S_k$, $x_f^{-1}(\underline{x})$ is well defined and contained in $\partial S_{\bar{k}}$.

Proof of Lemma 7.4

By contradiction. Given $\underline{x}^0 \in S_k$, suppose for all $T<\infty$ there exists $\bar{k}>0$ such that for all $\bar{\varepsilon}>0$, we can find an ε , $0<\varepsilon<\bar{\varepsilon}$ satisfying $s_\varepsilon(T,\underline{x}^0) \not\in S_{\bar{k}}$.

Now, by the results of [13] , $s_\varepsilon(t,\underline{x}^0)$ must converge uniformly to $s_0(t,\underline{x}^0)$ on $[0,T]$ as $\varepsilon \to 0^+$. So if we can find ε arbitrarily close to zero such that $s_\varepsilon(T,\underline{x}^0) \not\in S_{\bar{k}}$, it follows that $s_0(T,\underline{x}^0) \not\in$ interior of $S_{\bar{k}}$. Since this reasoning applies for all $T<\infty$, we may conclude that the positive limit set [21] of $s_0(t,\underline{x}^0)$ does not intersect the interior of $S_{\bar{k}}$.

The remainder of this proof follows the reasoning of lemma 5.2.81 of [21]. We have shown that $V(s_0(\cdot,\underline{x}^0))$ is a nonincreasing function bounded below by zero, therefore it has a definite limit as $t \to \infty$, which we denote c . Let L be the positive limit set of $s_0(\cdot,\underline{x}^0)$. The fact that $V(s_0(t,\underline{x}^0)) \to c$ as $t \to \infty$ implies $V(\underline{x})=c$ for all $\underline{x} \in L$. But the positive limit set must be invariant with respect to D , so $\dot{V}(\underline{x})=0$ for all $\underline{x} \in L$.

Now, $L \cap$ interior of $S_{\bar{k}} = \phi$, so in particular $\underline{x}^e \not\in L$. We can easily show that the largest invariant set of D for which $\dot{V}(\underline{x}) = 0$ is the point $\underline{x}^e$, yielding the desired contradiction . ▪

References

[1] M.Y. Akhtar, "Frequency Dependent Dynamic Representation of Induction Motor Loads", *Proc. IEE*, vol. 115, pp. 802-812, June 1968.

[2] P.M. Anderson and A.A. Fouad, **Power System Control and Stability** , Ames Iowa: Iowa University Press, 1977.

[3] T. Athay , R. Podmore and S. Virmani, "A practical Method for Direct Analysis of Transient Stability", *IEEE Trans. on Power App. and Systems*, vol. PAS-98, no. 2, pp. 573-584 , March/Apr. 1979.

[4] T. Athay and D.I. Sun , "An Improved Energy Function for Transient Stability Analysis", *Proc. of the International Symposium on Circuits and Systems*, Chicago, Apr. 27-29, 1981.

[5] A.R Bergen and D.J. Hill, "A Structure Preserving Model for Power System Transient Stability Analysis," *IEEE Trans. on Power App. and Systems*, vol. PAS-100, pp. 25-35 ,Jan. 1981.

[6] L.O. Chua, "Dynamic Nonlinear Networks: State of the Art", *IEEE Trans. on Circuits* and *Systems* , vol. CAS-27, no. 11, pp. 1059-1087, Nov. 1980.

[7] E.A. Coddington and N. Levinson,**Theory of Ordinary Differential Equations** , McGraw-Hill Book Company, New York, 1955.

[8] A.H. El-Abiad and K. Nagappan, "Transient Stability Regions for Multimachine Power Systems" , *IEEE Trans. on Power App. and Systems*, vol. PAS-85, no. 2, pp. 169-179, Feb 1966.

[9] A.A. Fouad and S.E. Stanton, "Transient Stability of a Multimachine Power System, Part I: Investigation of System Trajectories; Part II: Critical Transient Energy " , *IEEE Trans on Power App. and Systems*, vol. PAS-100, no. 7, pp. 3408-3424, July 1981.

[10] F.C. Hopensteadt, "Singular Perturbations on the Infinite Interval," *Transactions of the American Mathematical Society*, vol. 123 (1966), pp.521-535.

[11] IEEE/PES Committee Report, "System Load Dynamics-Simulation Effects and Determination of Load Constants", *IEEE Trans. on Power App. and Systems* , vol. PAS-93, no. 2, pp. 600-609, Mar./Apr. 1973.

[12] F. Illecito, A. Ceyhan, and G. Ruckstuhl, "Behavior of Loads During Voltage Dips Encountered in Stability Studies: Field and Laboratory Tests" , *IEEE Trans. on Power App. and Systems*, vol. PAS-91, no. 6, pp. 2470-2479, Nov./Dec. 1972.

[13] J.J. Levin and N. Levinson, "Singular Perturbations of Nonlinear Systems of Differential Equations and an Associated Boundary Layer Equation", *Journal of Rational Mechanics and Analysis*, vol. 3, pp. 247-270, 1959.

[14] N. Narasimhumurthi and M.T. Musavi, "A General Energy Function for Transient Stability of Power Systems", *IEEE Trans. on Circuits* and *Systems* , to appear.

[15] M. Ribbens-Pavella, P.G. Murthy, and J.L. Howard, "The Acceleration Approach to Practical Stability Domain Esimation in Power Systems", *Proc. of the IEEE Conference on Decision and Control*, pp. 471-477, Dec. 1981.

[16] W. Rudin, **Principles of Mathematical Analysis**, Third Edition, New York: McGraw-Hill Book Company, 1964.

[17] S.S. Sastry, C.A. Desoer, P.P. Varaiya, "Jump Behavior of Circuits and Systems", *IEEE Trans. on Circuits* and *Systems* , vol. CAS-28, no. 12, Dec. 1981.

[18] S.S. Sastry and P. Variaya, "Hierarchical Stability and Alert State Steering Control of Power Systems," *IEEE Trans. on Circuits* and *Systems* , vol. CAS-27, no.11, pp.1102-112, Nov. 1980.

[19] B. Stott, "Power System Dynamic Response Calculations," *Proceedings of The IEEE* vol. 67, no. 2, pp. 219-241, Feb. 1979.

[20] N.A. Tsolas, "Stability and Computer Simulation of Power Systems," PhD Disertation, University of California, Berkeley, October, 1983.

[21] M. Vidyasagar, **Nonlinear Systems Analysis**, Englewood Cliffs, N.J. : Prentice-Hall, Inc. , 1978.

[22] J.L. Willems and J.C. Willems, "The Application of Lyapunov Methods to the Computation of Transient Stability Regions for Multimachine Power Systems," *IEEE Trans. on Power App. and Systems*, vol. PAS-89, no. 5/6, pp. 795-801, May/June 1970.

[23] F.F. Wu and C-C. Liu, "Characterization of Power System Small Disturbance Stability with Models Incorporating Voltage Variation," submitted to *IEEE Trans. on Circuits* and *Systems*

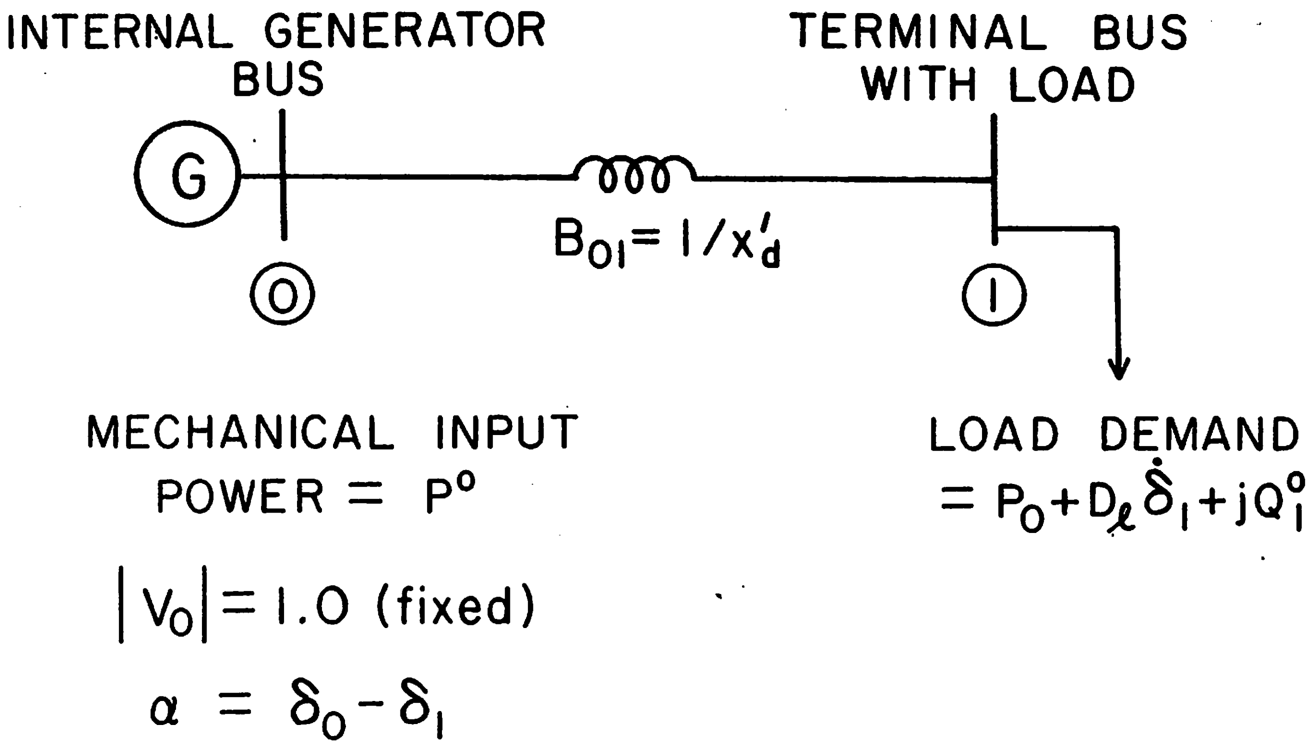
INTERNAL GENERATOR BUS
G
TERMINAL BUS WITH LOAD
$B_{01} = 1/x'_d$
0
1
MECHANICAL INPUT POWER = P^0
LOAD DEMAND $= P_0 + D_\ell \dot{\delta}_1 + jQ_1^0$
$|V_0| = 1.0$ (fixed)
$\alpha = \delta_0 - \delta_1$

Fig. 1

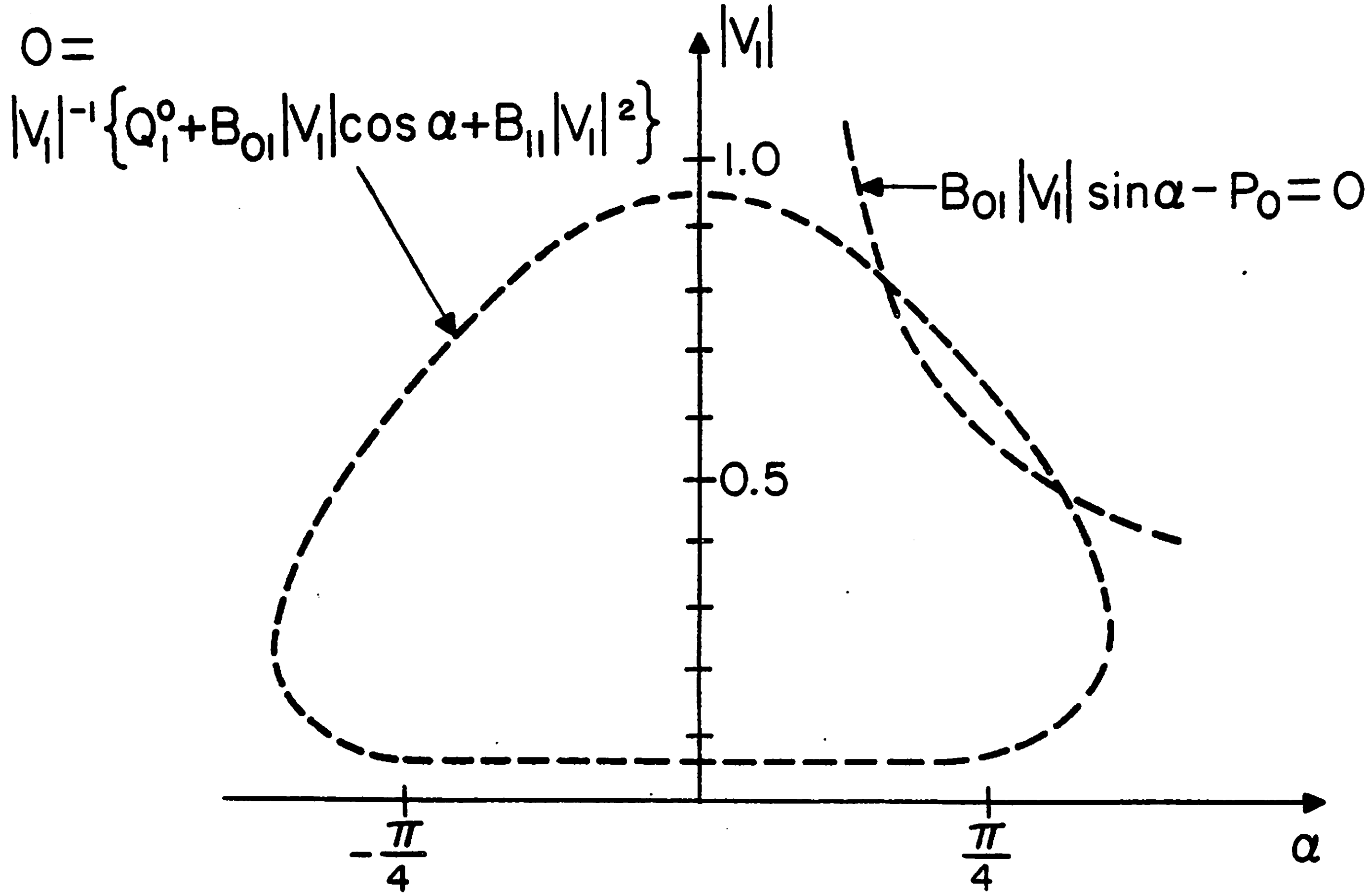

0 =
$|V_1|^{-1}\{Q_1^0 + B_{01}|V_1|\cos\alpha + B_{11}|V_1|^2\}$
$|V_1|$
1.0
0.5
$B_{01}|V_1|\sin\alpha - P_0 = 0$
$-\frac{\pi}{4}$
$\frac{\pi}{4}$
α

Fig. 2

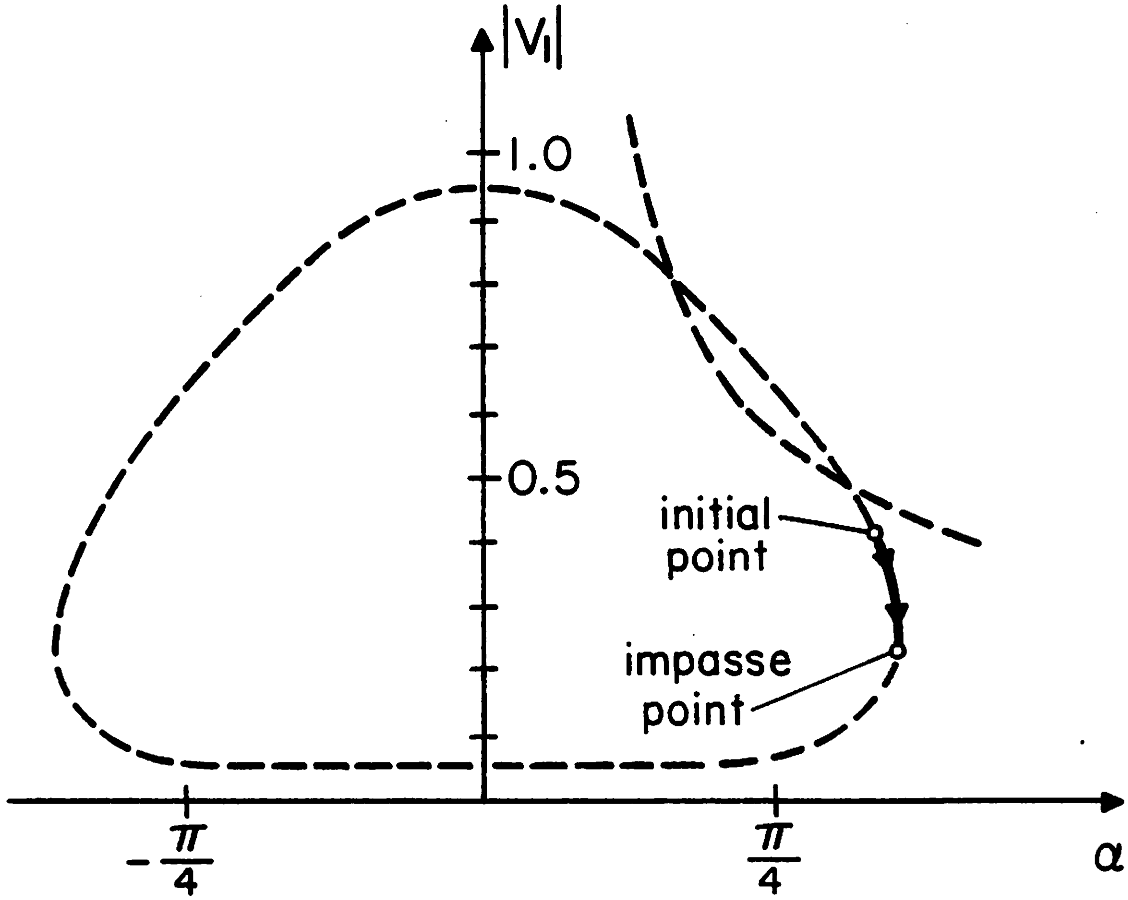

Fig. 3

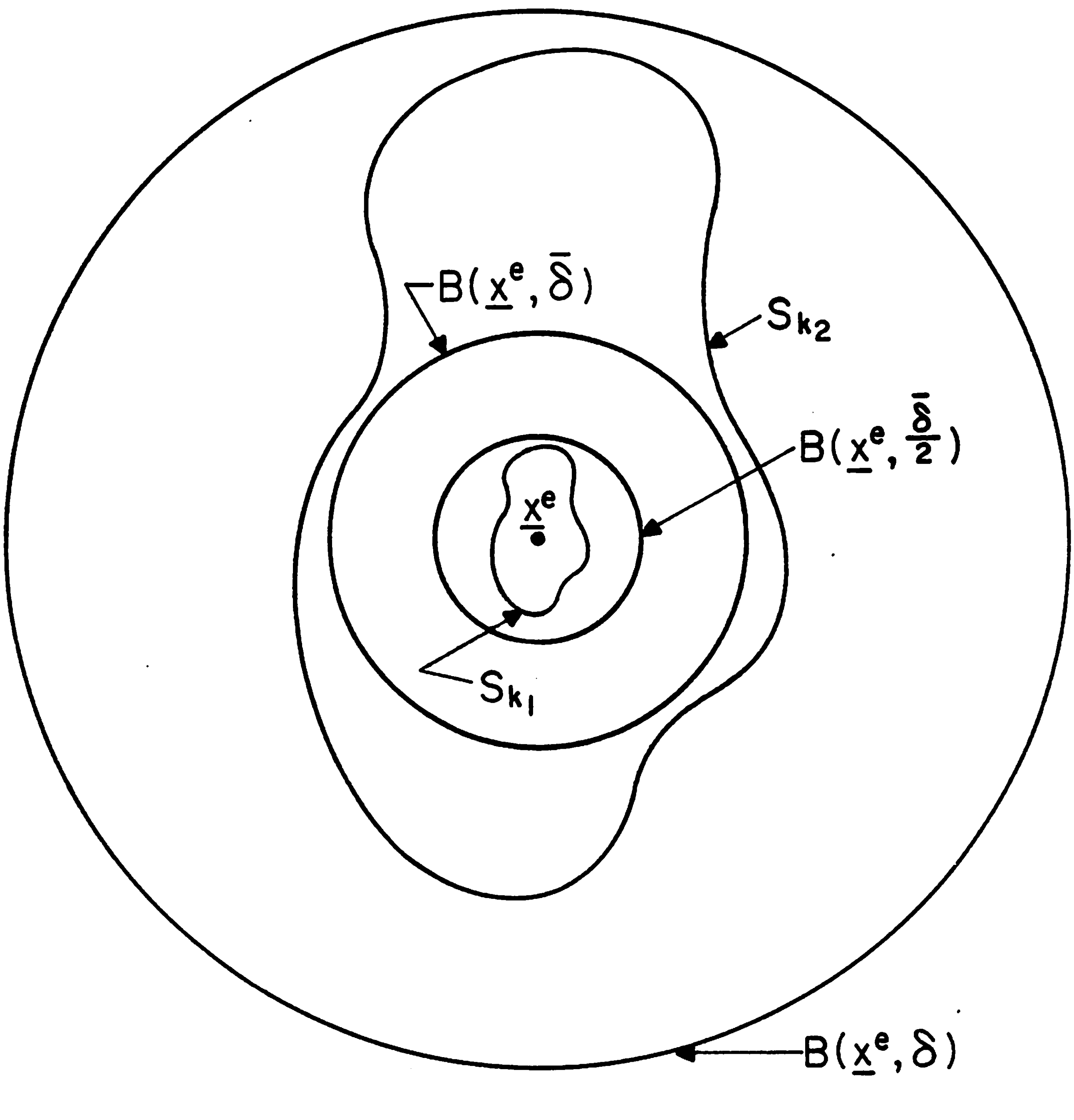

Fig. 4